

Denny, A.C., Fall, A., Orland, I.J., Valley, J.W., Eichhubl, P., and Laubach, S.E., 2019, A history of pore water oxygen isotope evolution in the Cretaceous Travis Peak Formation in East Texas: GSA Bulletin, <https://doi.org/10.1130/B35291.1>.

Data Repository

Appendix A

Appendix B

Appendix C. Method used to determine that intersected fluid inclusions do not affect SIMS values in quartz.

Appendix D1

Appendix D2

Appendix E. Burial Model and Sensitivity Analysis.

Appendix C - Method used to determine that intersected fluid inclusions do not affect SIMS values in quartz

Included in Denny et al., 2019: A History of Pore Water Oxygen Isotope Evolution in the Cretaceous Travis Peak Formation.

Contents

1. Introduction: SIMS Procedure and Pit Evaluation	1
Figure C1. A backscattered electron SEM image of a sub-region of quartz bridge SFE2, taken after SIMS analysis.	2
2. Comparing Pit Morphologies to Measured OH⁻	3
Figure C2 (OH⁻ cps compared to SEM pit inspection). Histogram of analysis averaged OH ⁻ (Gcps).	3
Figure C3 (background-corrected OH⁻ compared to SEM pit inspection). Histogram of background-corrected OH ⁻ /O counts (i.e., normalized to background determined from the bracketing UWQ-1 standard).	4
3. Comparing Pit Morphologies to Count-Rate Behavior	4
3.1 Count-Rate Behavior: Regular Quartz Pits	4
Figure C4 (regular pit shape). Plots of cycle-by-cycle OH ⁻ and ¹⁶ O ⁻ counts, from analysis #651, a pit which had a regular shape under SEM (Figure C1).	5
3.2 Count Rate Behavior: Irregular Pits (Groups 1 and 2).....	5
Figure C5 (irregular pit shape, Group 1). Plots of cycle-by-cycle OH ⁻ and ¹⁶ O ⁻ ion counts for a mixed-phase analysis, from analysis #648.	6
Figure C6 (irregular pit shape, Group 2). Plots of cycle-by-cycle OH ⁻ and ¹⁶ O ⁻ ion counts for a suspected fluid inclusion interception, from analysis #646. This	7
3.3 Evaluating OH ⁻ Spike δ ¹⁸ O Values.....	7
Figure C7. Method used to determine whether spikes in OH ⁻ counts affect δ ¹⁸ O values.	8
Figure C8. Calculated average δ ¹⁸ O values of bracketing OH ⁻ cycles plotted against calculated δ ¹⁸ O values of individual high OH ⁻ cycles.	9
3.4 A Note Concerning the Feasibility of Fluid Inclusion δ ¹⁸ O _{water} Measurements.....	9

1. Introduction: SIMS Procedure and Pit Evaluation

During SIMS analysis on quartz, simultaneous measurement was made of the ¹⁸O⁻, ¹⁶O⁻, and ¹⁶O¹H⁻ ions (for additional details concerning instrumental conditions, see the methods). Because the ¹³³Cs⁺ beam sputtering required to produce these ions is a continuous process, ion counts on the detectors were summed into 20 bins, or “cycles”, of four seconds each to help track conditions during

pit excavation. The $^{16}\text{O}^1\text{H}^-$ ion, hereafter referred to as OH^- for simplicity, is measured to help verify that hydrous or organic phases were not intersected during analysis; increases in this count rate above background can be a potential indicator of phase alteration, contamination, or mixed-phase analyses.

Post-SIMS imaging by SEM of SIMS pits is regularly undertaken by the WiscSIMS lab to verify that analyses were at locations of interest and to ascertain that pits have a “normal” or “regular” appearance. If a pit intersects a crack or different phase during analysis, the crack or intersected phase can commonly be observed by SEM. For this study, post-analysis imaging revealed small (often $<1\ \mu\text{m}$) empty voids in the bottoms of some of the quartz pits, resulting in “irregular” pit morphologies (Figure C1). These pockets are interpreted to result from fluid inclusions intersected during pit excavation.

At the time of data collection, it was unknown whether the vapor released from intercepted fluid inclusions could significantly affect ionization of a particular isotope, or whether the liberated fluid itself would be ionized and affect the measured $\delta^{18}\text{O}$ value of the analysis. **As will be demonstrated below, analyses that intersect fluid inclusions do not significantly affect measured $\delta^{18}\text{O}$ values on quartz, provided they are not large enough to adversely affect the overall pit shape.**

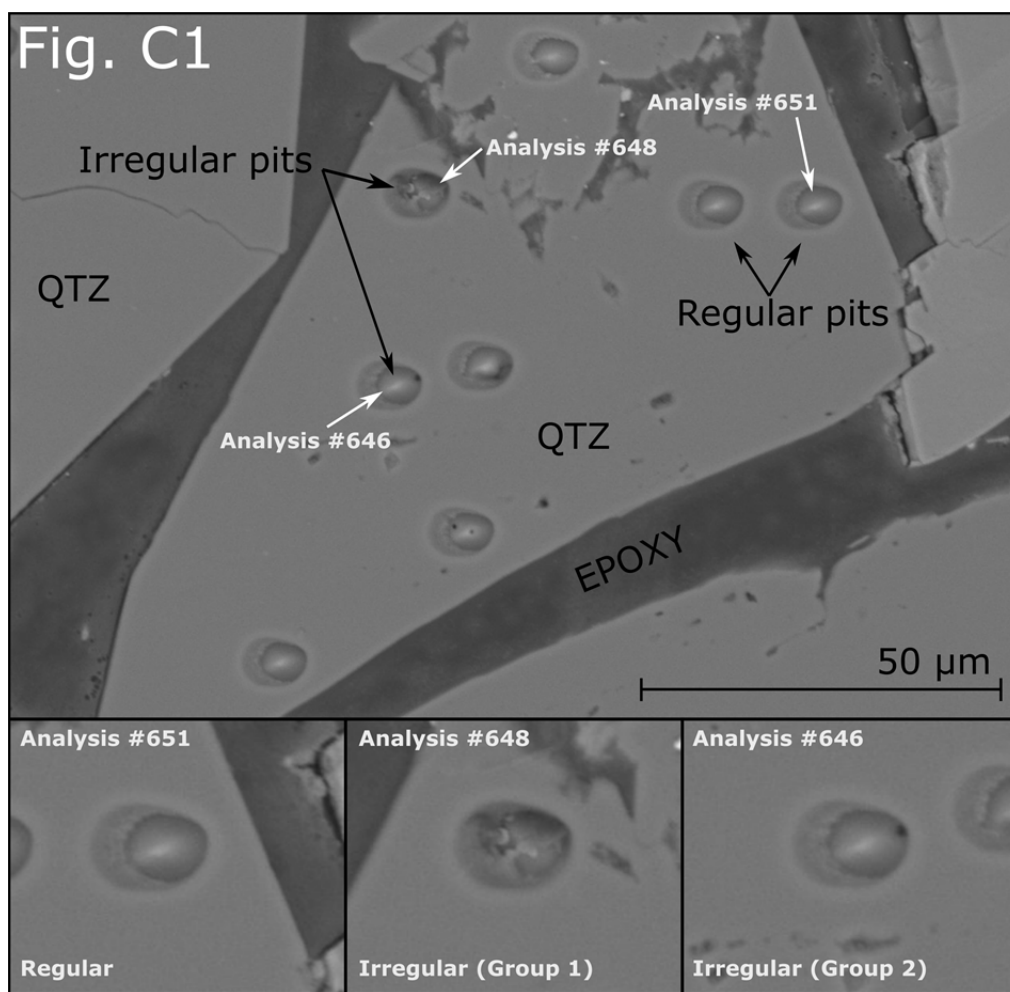


Figure C1. A backscattered electron SEM image of a sub-region of quartz bridge SFE2, taken after SIMS analysis. Quartz (light grey phase), epoxy (dark grey phase), and several SIMS analysis pits are evident. Examples of both regular and the two irregular pit types observed are shown in finer detail.

2. Comparing Pit Morphologies to Measured OH⁻

Visual inspection of SIMS pits by SEM allowed for the classification of pits according to whether they were visibly pristine in shape, had intersected cracks or epoxy or other mineral phases, or had visible holes in their bottoms. Here those classifications are compared to two SIMS parameters commonly used to weed out problematic or erroneous analyses: $^{16}\text{O}^1\text{H}/^{16}\text{O}$ counts per second (Fig. 2), and background-normalized $^{16}\text{O}^1\text{H}/^{16}\text{O}$ (Fig. C3). Broadly speaking, discarding analyses with high OH⁻ counts is an effective means of eliminating potentially erroneous data. However, here it does not succeed in capturing all of the analyses exhibiting non-pristine pit shapes or strange cycle-by-cycle OH⁻ behavior. This demonstrates the value of complimentary SEM pit inspection (e.g., Fig. C1) and cycle-by-cycle evaluation of individual analyses (following sections) in creating robust and reproducible SIMS datasets. Be aware that holes as classified here are not uniform in size from pit to pit, and so a single large hole may represent greater liberated volume than several small ones.

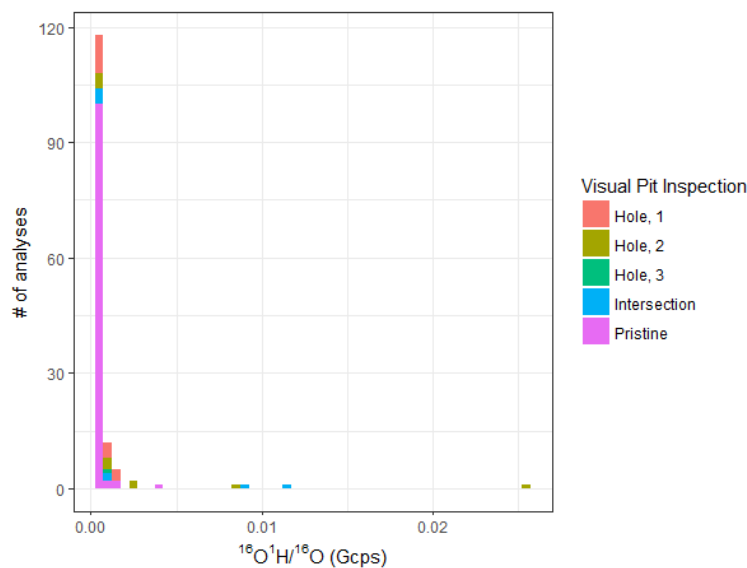


Figure C2 (OH⁻ cps compared to SEM pit inspection). Histogram of analysis averaged OH⁻ (Gcps). Analyses are classified according to whether in SEM imagery they had a pristine appearance (“Pristine”), visibly intersected a separate mineral/epoxy phase (“Intersection”), or had 1 to 3 visible holes in the pit bottom thought to originate from intersected fluid inclusions (“Hole 1, 2, 3”).

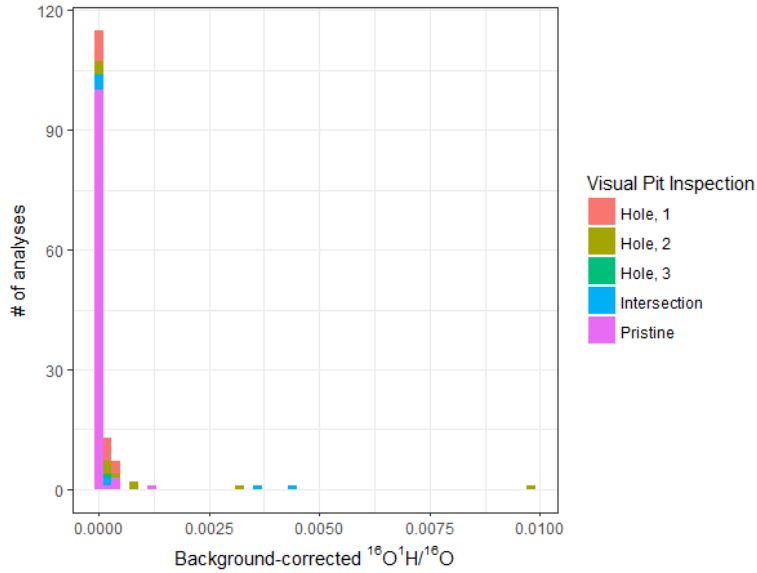


Figure C3 (background-corrected OH compared to SEM pit inspection). Histogram of background-corrected OH/O counts (i.e., normalized to background determined from the bracketing UWQ-1 standard). Analyses are classified according to whether in SEM imagery they had a pristine appearance (“Pristine”), visibly intersected a separate mineral/epoxy phase (“Intersection”), or had 1 to 3 visible holes in the pit bottom thought to originate from intersected fluid inclusions (“Hole 1, 2, 3”).

3. Comparing Pit Morphologies to Count-Rate Behavior

3.1 Count-Rate Behavior: Regular Quartz Pits

Testing whether the liberation of fluid inclusions affects $\delta^{18}\text{O}$ values requires looking at the cycle-by-cycle count rates (i.e., the 20 four-second cycles that comprise one analysis). An example of these count rates for a regularly-shaped SIMS pit on quartz can be found in Figure C4. Some background OH^- ion counts and variability are expected due to sample degassing and evolving conditions in the sample chamber. Under the operating conditions in which this paper’s quartz data were collected, OH^- ion count rates between 3×10^5 and 5×10^5 counts per second were typical for quartz standard UWQ-1. This range thereby reflects the expected OH^- background for regular quartz analyses. Because UWQ-1 is derived from a granulite facies quartzite, the quartz contribution to OH^- counts is assumed to be negligible, and so most of this background signal likely results from sample degassing and adsorbed molecules.

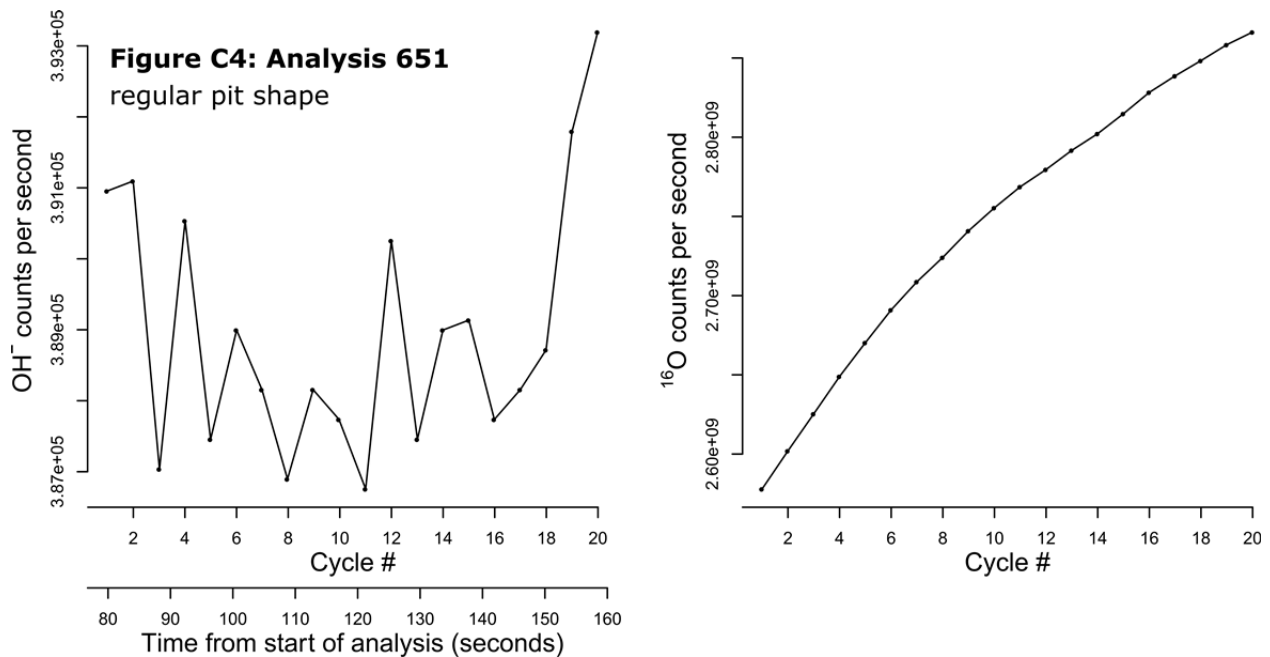


Figure C4 (regular pit shape). Plots of cycle-by-cycle OH⁻ and ¹⁶O⁻ counts, from analysis #651, a pit which had a regular shape under SEM (Figure C1). Counts rates of ¹⁶O⁻ (shown above) and ¹⁸O⁻ (not shown, but similar in trend) increase steadily and consistently during the counting time of regular analyses. This increase in ¹⁶O count rate is common in quartz and affects ¹⁸O proportionately, such that the isotope ratio is minimally perturbed over the duration of measurement.

3.2 Count Rate Behavior: Irregular Pits (Groups 1 and 2)

Analyses containing deviations from background values can be placed into two groups. The first group, an example of which is given in Figure C5 below, constitutes analyses showing prolonged, progressive changes in cycle-by-cycle OH⁻ counts. The second group, an example of which is given in Figure C6 below, constitutes analyses showing short, punctuated spikes in cycle-by-cycle OH⁻ counts that last no longer than 1-3 cycles (4-12 s) before returning to background values, with the largest spikes in OH⁻ count rate showing the slowest attenuation. It is this latter group of short, punctuated OH⁻ excursions that is thought to originate from the release of fluid inclusions during SIMS pit excavation.

Post-SIMS SEM imagery was conducted on the pits excavated by analyses exhibiting both types of OH⁻ behavior. Images associated with prolonged OH⁻ excursions (Group 1) indicated that pit excavation had either intersected a crack in quartz or had excavated down to a non-quartz phase that was previously hidden below the surface. Images associated with punctuated OH⁻ spikes (Group 2, suspected fluid inclusions) typically still had small empty intersected pockets visible in the pit bottoms.

Group 1 trends commonly also show significant deviations in ¹⁸O and ¹⁶O, as well as ¹⁸O/¹⁶O ratios, coincident with deviations in OH⁻ values. Because Group 1 trends were interpreted to represent mixed-phase analyses, they were excluded from further OH⁻ analysis, and were not used to construct the interpretations made in this paper.

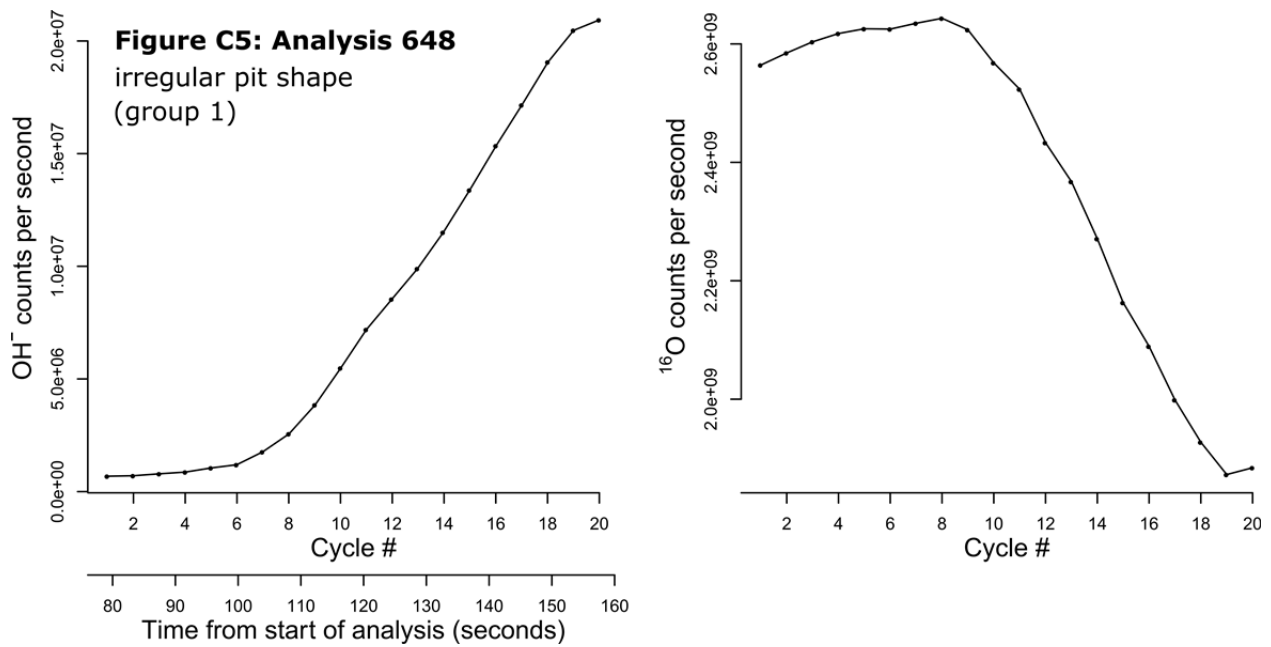


Figure C5 (irregular pit shape, Group 1). Plots of cycle-by-cycle OH⁻ and ¹⁶O⁻ ion counts for a mixed-phase analysis, from analysis #648. This pit has an irregular shape in SEM imaging, displaying overall the typical oval shape but with an uneven bottom suggesting that a planar feature was intersected during analysis (Figure C1). This analysis started on pure quartz, but appears to have intercepted a crack or a different phase before Cs⁻ sputtering was completed. The counts of OH⁻ display a trend that can be ascribed to mixing between quartz and a phase richer in OH. As more and more of the new phase was exposed as the sputtering process excavated the pit, the OH⁻ counts rose accordingly. Note that OH⁻ counts rise to nearly two orders of magnitude above quartz background by the end of the analysis at cycle 20. Counts on ¹⁶O⁻ (shown above) and ¹⁸O⁻ (not shown, but similar in trend) are perturbed progressively lower as OH⁻ counts increase. The intercepted phase is not known for certain, but energy dispersive x-ray spectroscopy of the pit bottom indicates the presence of K and Al, suggesting that the phase is a clay or similar alteration mineral.

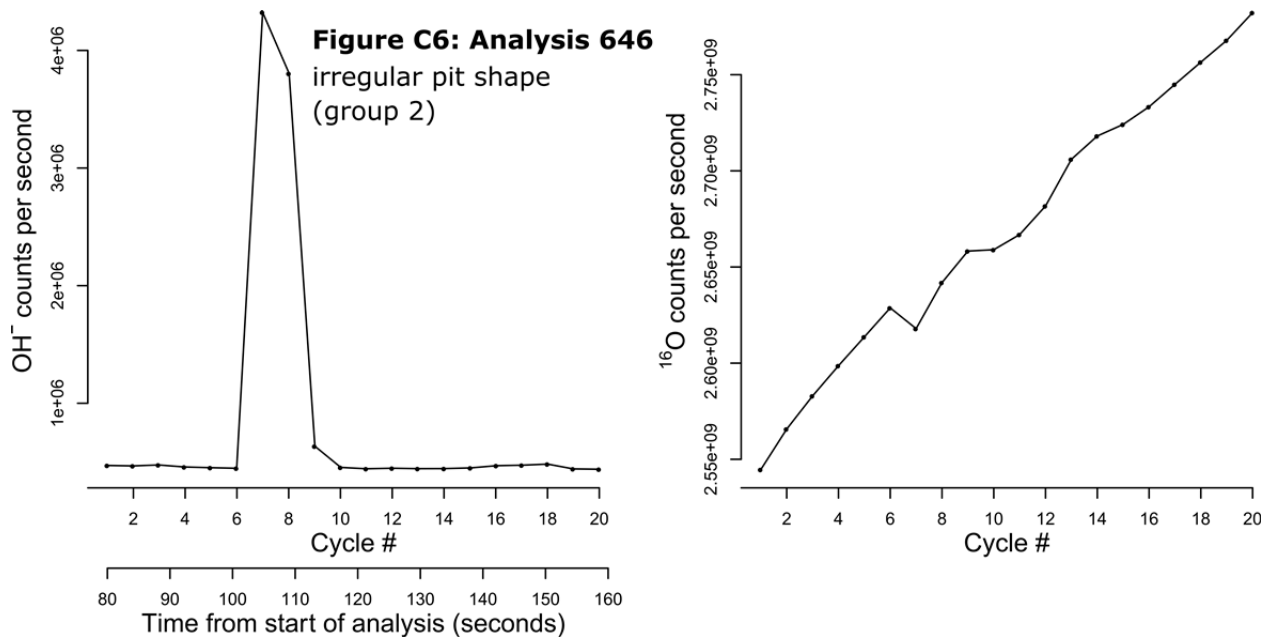


Figure C6 (irregular pit shape, Group 2). Plots of cycle-by-cycle OH⁻ and ¹⁶O⁻ ion counts for a suspected fluid inclusion interception, from analysis #646. This pit has an otherwise regular shape under SEM, with the exception of a small pocket in the pit's upper right (Figure C1). Note that OH⁻ counts rise to an order of magnitude above quartz background for two cycles before returning to typical quartz background values. Such a short pulse of OH⁻ is difficult to ascribe to an intercepted phase unless that phase were easily volatilized and contains a high concentration of OH bonds. Counts on ¹⁶O⁻ (shown above) and ¹⁸O⁻ (not shown, but similar in trend) are perturbed lower at the onset of the OH⁻ spike, but quickly return to the climb in count rates typical of regular quartz analyses (Figure C4).

3.3 Evaluating OH⁻ Spike δ¹⁸O Values

Of the 130 sample analyses remaining after the removal of irregular pit shapes and analyses exhibiting Group 1 behavior, 33 had aberrant OH⁻ spikes that placed them in Group 2. To test if Group 2 OH⁻ spikes had an effect on final δ¹⁸O values, a method was devised by which uncorrected δ¹⁸O values would be calculated for every cycle containing OH⁻ count rates above a certain threshold (here chosen to be 8×10⁶ counts per second). That value would then be compared to the uncorrected δ¹⁸O average of the cycles below the OH⁻ threshold on either side of the OH⁻ spike (Figure C7).

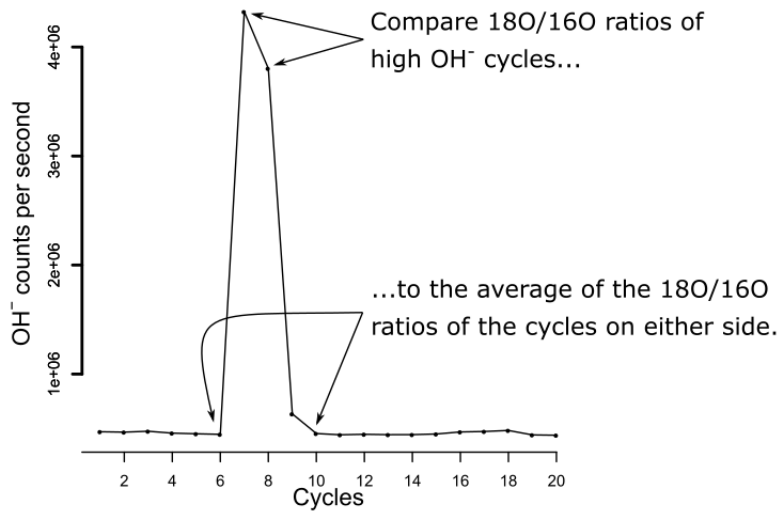


Figure C7. Method used to determine whether spikes in OH⁻ counts affect $\delta^{18}\text{O}$ values. The results of this method are presented in Figure C8 (below).

If the spikes in OH⁻ count rate from intersecting fluid inclusions do not affect $\delta^{18}\text{O}$ values, then there should be little to no difference between the uncorrected $\delta^{18}\text{O}$ values for OH⁻ spike cycles and the uncorrected $\delta^{18}\text{O}$ values for cycles on either side of the OH⁻ spike. Plotting one versus the other for all Group 2 quartz analyses on the sample, we can see that the data closely follow a 1:1 line (Figure C8, below). This indicates that transient OH⁻ spikes during analysis do not significantly bias $\delta^{18}\text{O}$ analysis values, and so these analyses may be included in the final interpretation.

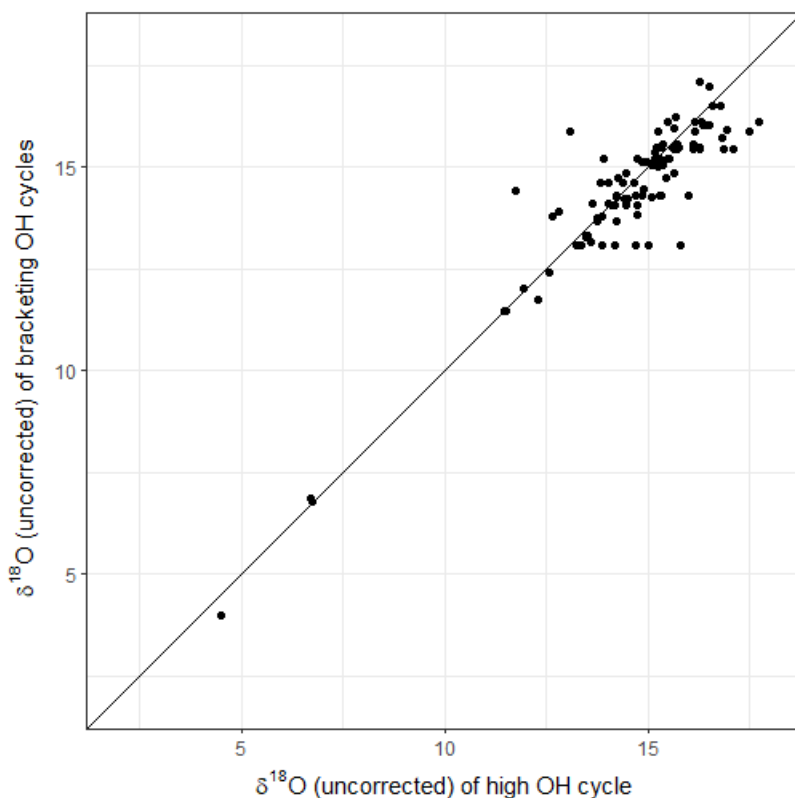


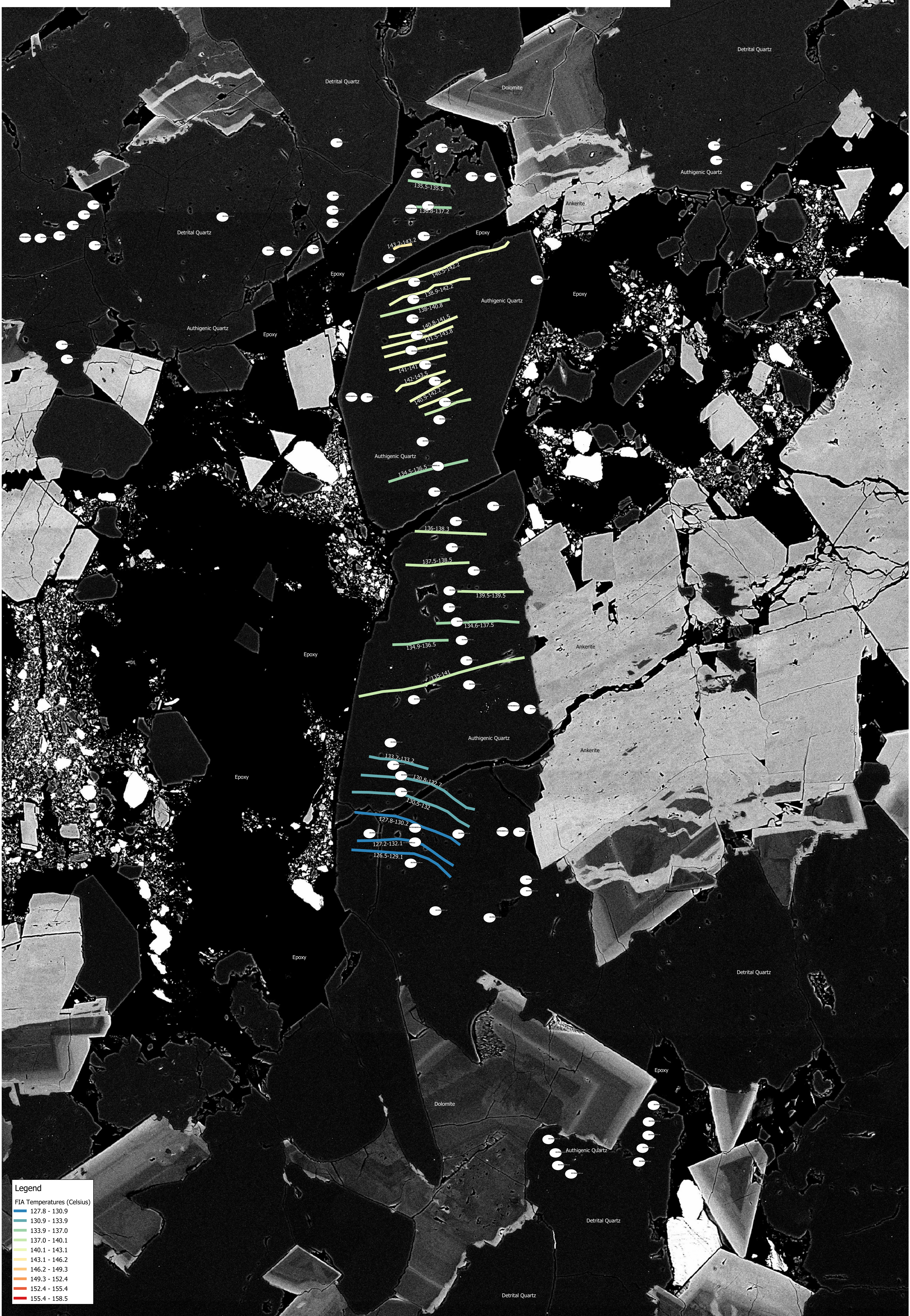
Figure C8. Calculated average $\delta^{18}\text{O}$ values of bracketing OH cycles plotted against calculated $\delta^{18}\text{O}$ values of individual high OH cycles. The slope = 1, intercept = 0 line plotted through the data indicates that inclusion-derived punctuated OH spikes do not significantly affect $\delta^{18}\text{O}$ values, provided there is no associated change in mineral phase. Note that these $\delta^{18}\text{O}$ values represent raw ratios directly from the instrument and have not been corrected to their bracketing standards; therefore, they are lower than what the quartz's true value would be. Precision is degraded for $\delta^{18}\text{O}$ if measured on the basis of only two cycles, which is the cause of some of the scatter about the 1:1 line.

3.4 A Note Concerning the Feasibility of Fluid Inclusion $\delta^{18}\text{O}_{\text{water}}$ Measurements

The data above might imply to the reader that SIMS may be a potential way to measure fluid inclusion $\delta^{18}\text{O}_{\text{water}}$ values in the future. However, there are several analytical challenges that would first have to be overcome before this is feasible. The main problem is that there is no way to know without some standardization method that $^{18}\text{O}^1\text{H}$ and $^{16}\text{O}^1\text{H}$ are ionized with equal efficiency when these inclusions are penetrated. If one could create or find a sample with fluid inclusions of known $\delta^{18}\text{O}$ compositions in quartz, and demonstrate that they behave in a predictable fashion during analysis, and further demonstrate that additional factors such as inclusion chemistry do not affect measurements, then this could become a useful technique for measuring $\delta^{18}\text{O}$ of inclusions. As for the data presented in the manuscript, we only measured $^{16}\text{O}^1\text{H}$, and so cannot evaluate this question further.

SFE2 (BSE imagery, no CL)

0 50 100 150 200 μm



SFE2 (composite color CL)

0 50 100 150 200 μm

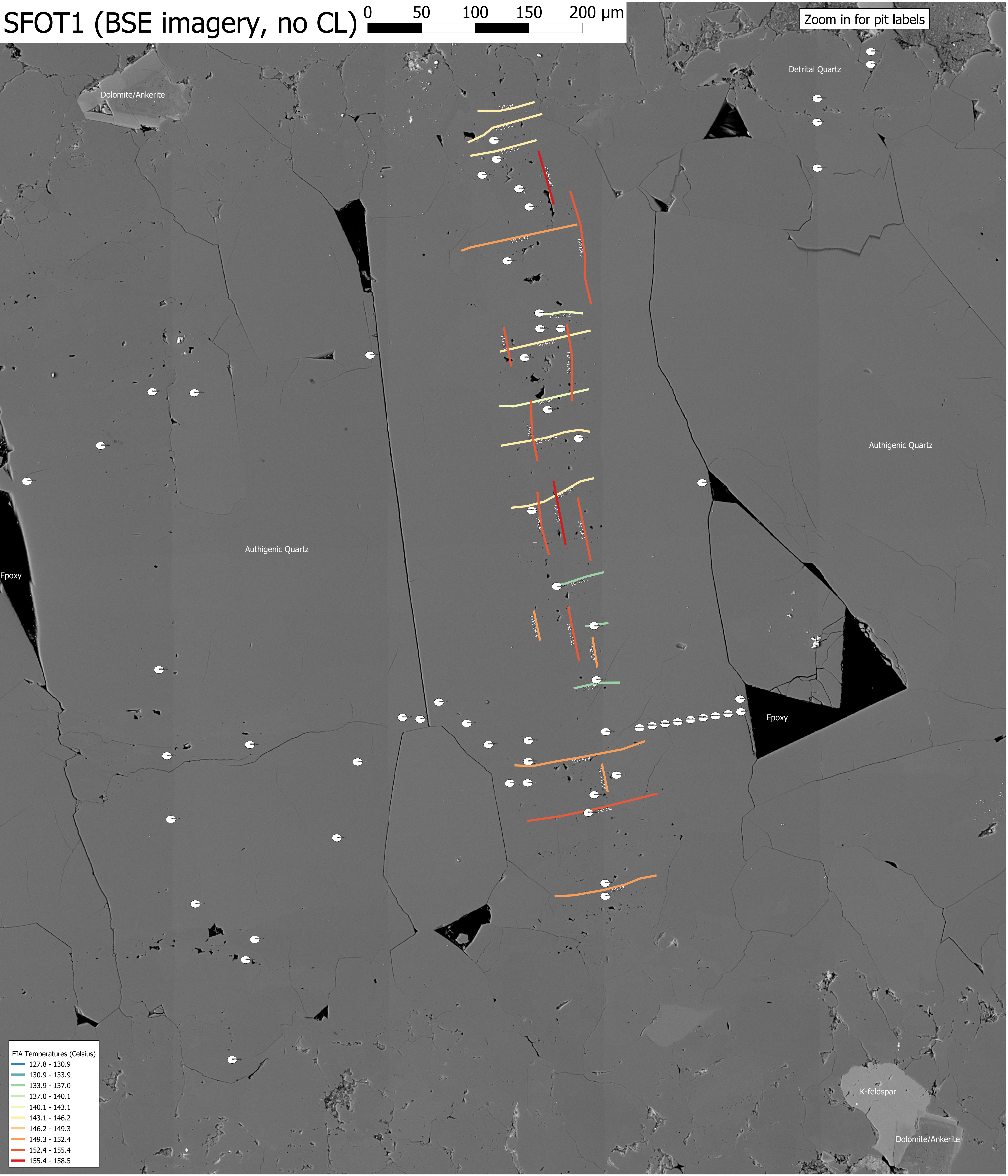


Legend

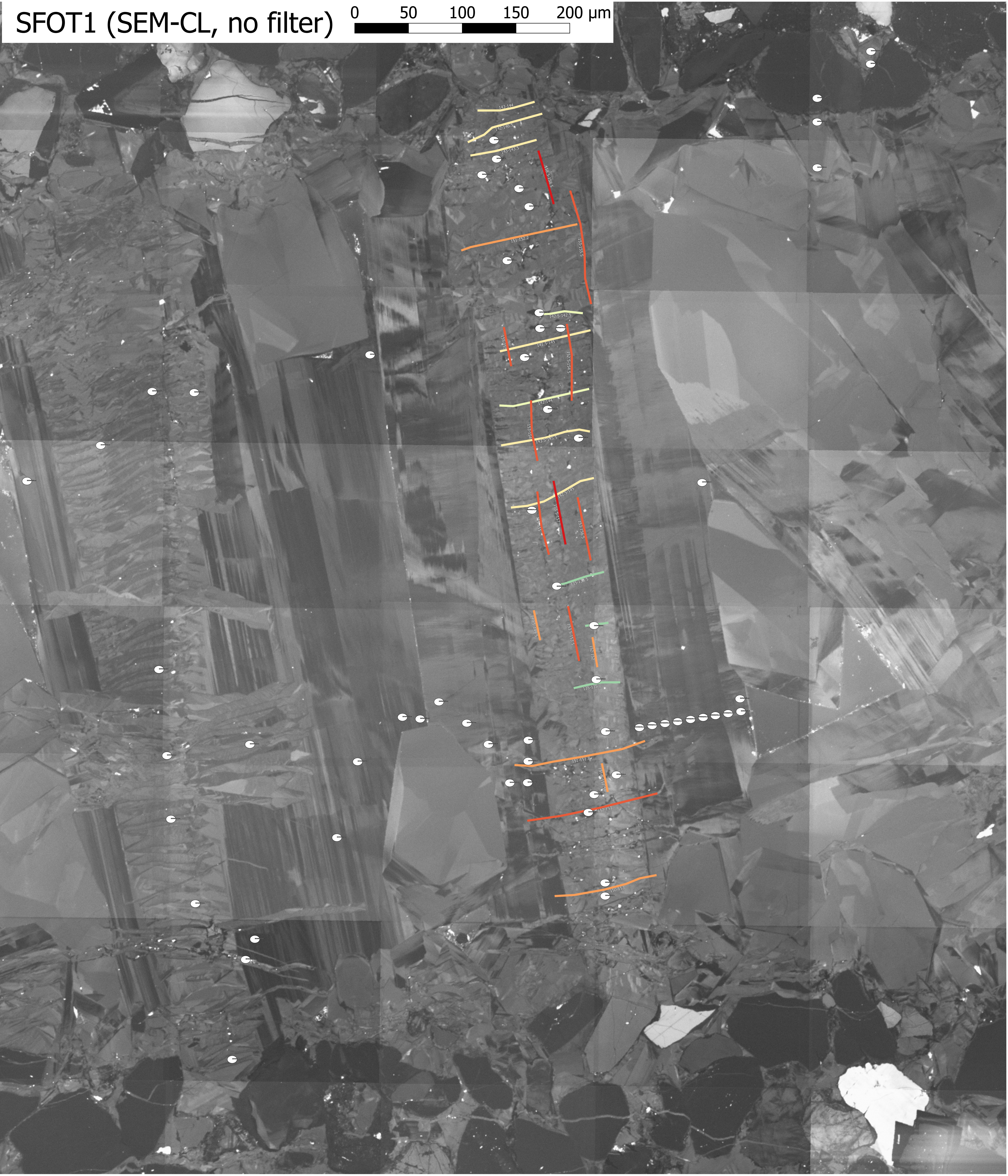
FIA Temperatures (Celsius)

127.8 - 130.9
130.9 - 133.9
133.9 - 137.0
137.0 - 140.1
140.1 - 143.1
143.1 - 146.2
146.2 - 149.3
149.3 - 152.4
152.4 - 155.4
155.4 - 158.5

SFOT1 (BSE imagery, no CL) 0 50 100 150 200 μm



SFOT1 (SEM-CL, no filter) 0 50 100 150 200 μm



Appendix E – Burial Model and Sensitivity Analysis

Included in Denny et al., 2019: A History of Pore Water Oxygen Isotope Evolution in the Cretaceous Travis Peak Formation.

Contents

Introduction	1
Model Overview	1
Model Sensitivity to Varying Parameters	3
Depth Increment ('depth_increment' parameter)	4
Initial Porewater $\delta^{18}\text{O}$ Value ('init_wat_d18o' parameter)	5
Initial Quartz $\delta^{18}\text{O}$ Value ('init_detmin_d18o' parameter)	6
Portion of Dissolving Cement vs. Dissolving Detrital Quartz ('cem_diss_prop' parameter)	7
Geothermal Gradient ('INPUT_geotherm' parameter)	8
Mechanical Compaction and Pressure Solution of Quartz ('INPUT_mech' parameter)	9
No Matches Found for All Possible Closed-System Conditions	10

Introduction

Additional information is included in this appendix regarding the R model constructed to simulate our observations (the full R code is available in Appendix F). First, a more detailed discussion of the model is given, with its strengths and weaknesses highlighted. This is followed by several examples to demonstrate model sensitivity in response to varying input parameters.

Model Overview

In the model, it is assumed that the change in porosity in quartz-rich sandstones over a small change in burial depth can be broken down into 3 components reflecting 3 different compactional processes: 1) mechanical compaction m , 2) grain boundary pressure solution p , and 3) quartz cement precipitation Qtz_{cem} , such that:

$$\Delta\Phi = m + p + Qtz_{cem} \quad [1]$$

Only the pressure solution and cementation will have an impact on porewater $\delta^{18}\text{O}$ values; mechanical compaction processes do not play a direct role. The pressure solution term p may be further broken down into the portion of mineral p_{min} dissolved during pressure solution, and the portion of porosity lost to pressure solution volume change p_{pore} (see figure below). If there is no net loss or gain in silica, then the cement precipitation term Qtz_{cem} and the p_{min} term become equivalent to each other, which means that for any change in porosity from initial porosity Φ_n to new post-compaction porosity Φ_{n+1} , the following relationship may be defined:

$$\Phi_n = \Phi_{n+1} + m + p_{pore} + p_{min} \quad [2]$$

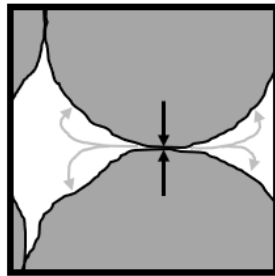
If the rate of change in porosity with depth, the proportion of that change which is due to mechanical compaction, and the relative contributions of p_{pore} and p_{min} to pressure solution p are known for a formation, then it follows that the volume of silica chemically interacting with the porewater through the process of pressure solution and cementation can be estimated. In the absence of fluid infiltration, the interaction between silica and porewater will be the sole driver of $\delta^{18}\text{O}_{\text{water}}$ trends in pure quartz sandstones.

A particular challenge with this approach is determining the relative importance of p_{pore} and p_{min} at any given depth. The model takes the simplifying assumption that these terms are ratioed to porosity such that for any small change in porosity with burial depth:

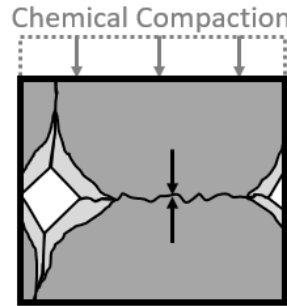
$$p_{min} = (1 - \Phi_n) * p \quad [3]$$

(a) Sandstone Chemical Compaction

depth = 0 (sand)

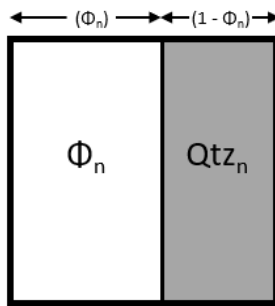


depth >> 0

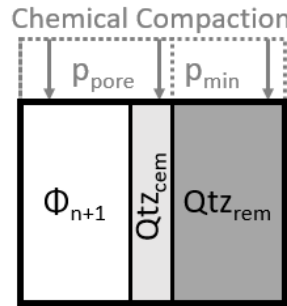


(b) Computational Burial Model

depth = n



depth = n + 1



$$Qtz_n = Qtz_{n+1} = Qtz_{cem} + Qtz_{rem}$$

$$Qtz_{cem} = p_{min}$$

This relationship is shown visually in the figure above. In this way, the contribution of p_{pore} to porosity loss scales linearly with % porosity. It should be noted, however, that Eqn. 3 does not truly reflect the spatial relationship between sand grains, as the rounded morphology of grains that is common in sandstones will lower the value of p_{min} below that shown in Eqn. 3, particularly during the early stages of burial compaction. This simplifying assumption avoids the difficult spatial problem of determining numerically what the values of p_{pore} and p_{min} will be for a variety of grain orientations, grain shapes, and grain size distributions, at a variety of stages in burial evolution. The result of using Eqn. 3 will be an overestimate of the amount of quartz that interacts with the fluid during pressure solution and cementation, making the model output an upper bound for internally mobilized silica.

At each iteration of the model, oxygen atoms from the quartz dissolved at grain boundaries are allowed to fully mix with the oxygen in the water, changing the $\delta^{18}O_{porewater}$ value accordingly, before a volume of quartz cement is precipitated that is equivalent to the volume of quartz initially dissolved at the grain boundaries. The $\delta^{18}O$ value of the newly precipitated overgrowth quartz is calculated using the quartz-water equilibrium fractionation (Clayton et al., 1972; Friedman and O'Neil, 1977) and the temperature gained from a geotherm curve as an additional input.

Particularly thick sequences of sandstone (such as those in the Travis Peak) or regionally extensive sandstones which have experienced a range of maximum burial depths can provide sufficient porosity data for extrapolation. The

proportion of porosity lost to mechanical compaction is difficult to determine observationally, but a reasonable estimate can be made by comparing porosity data to intergranular volume (IGV) data, and filling in gaps in knowledge with data from analogous formations.

Excess water is assumed to be expelled from the system laterally, with no vertical mixing or significant transport of pore fluids. This first-order approximation of fluid removal is reasonable for sandstones where formation-perpendicular movement through the formation is more restricted than formation-parallel movement, and where faulting or other structures provide conduits for rapid removal of compaction-driven water to leave the system and head towards the surface. No significant overpressuring effect is assumed in the model.

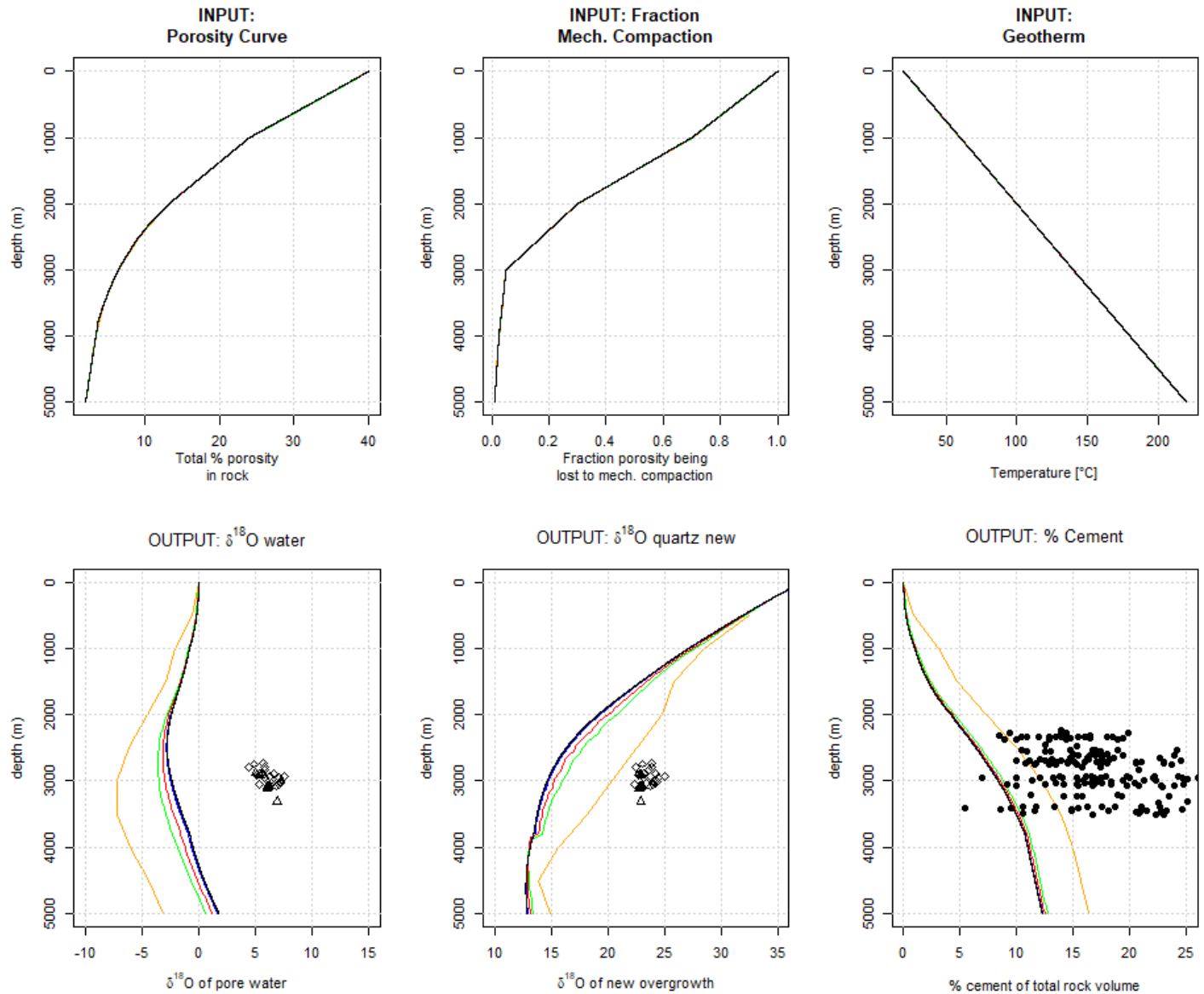
Model Sensitivity to Varying Parameters

In each of the following examples, several variants on each input parameter will be given to demonstrate the model's sensitivity. The best estimate model presented in the paper in Figures 10 and 11 (denoted by the black line) will be the same in each of the plots below to aid in comparison.

Depth Increment ('depth_increment' parameter)

Running the model with a large depth increment introduces inaccuracy to the result, as this makes the number of calculations insufficient to approach the equilibrium state between pore fluid and mineral phases. Deviation of model results between different runs of different depth increments is minimal for depth increments of 10 m or less, demonstrating that increments in this range produce the most accurate model results.

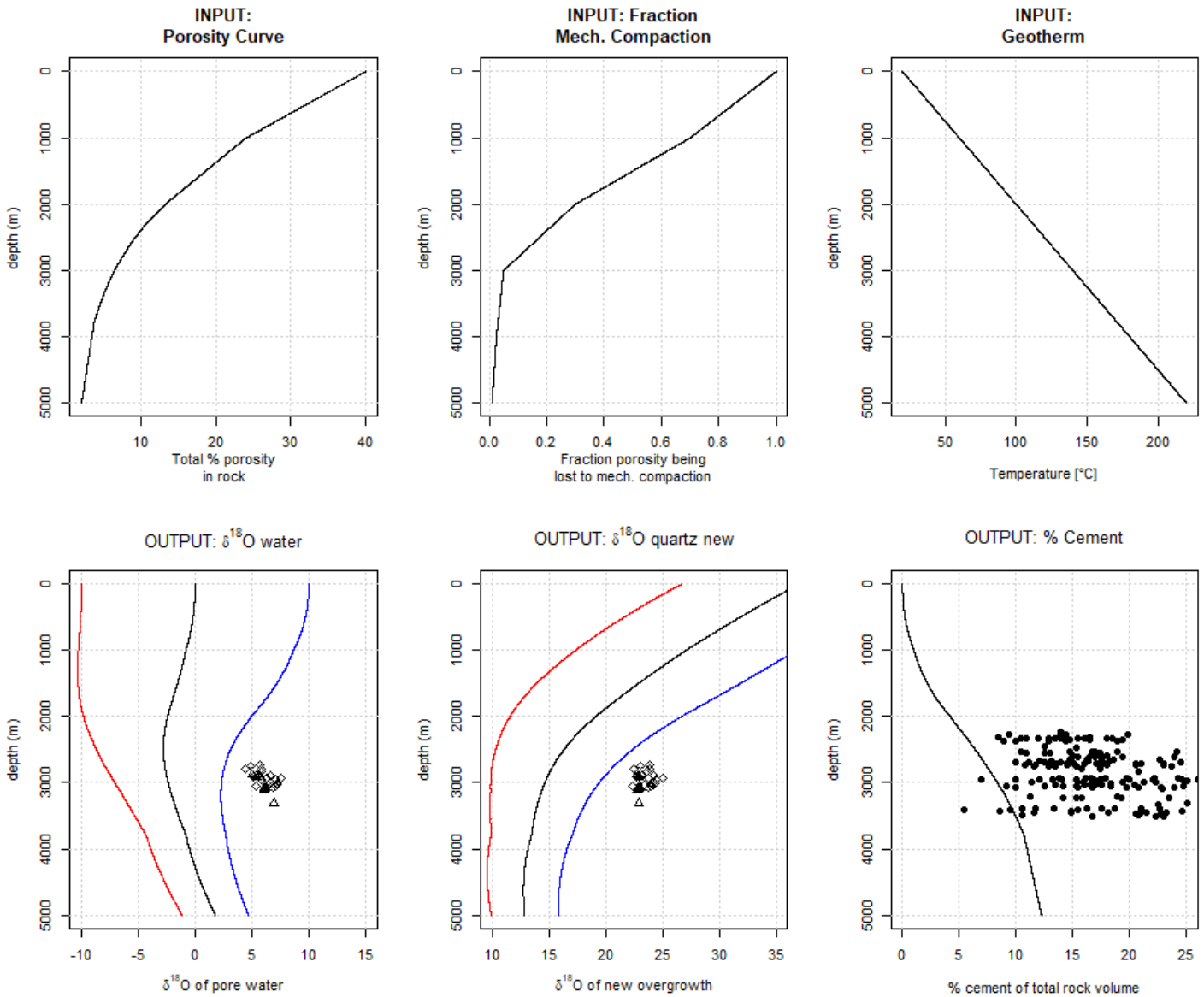
- **BLACK** => depth_increment = 1 m
- **BLUE** => depth_increment = 10 m
- **RED** => depth_increment = 50 m
- **GREEN** => depth_increment = 100 m
- **ORANGE** => depth_increment = 500 m



Initial Porewater $\delta^{18}\text{O}$ Value ('init_wat_d18o' parameter)

The initial $\delta^{18}\text{O}$ value of the porewater can be set for a model run, and below is shown how changing this value to higher or lower initial $\delta^{18}\text{O}_{\text{porewater}}$ might affect the trajectory of porewater.

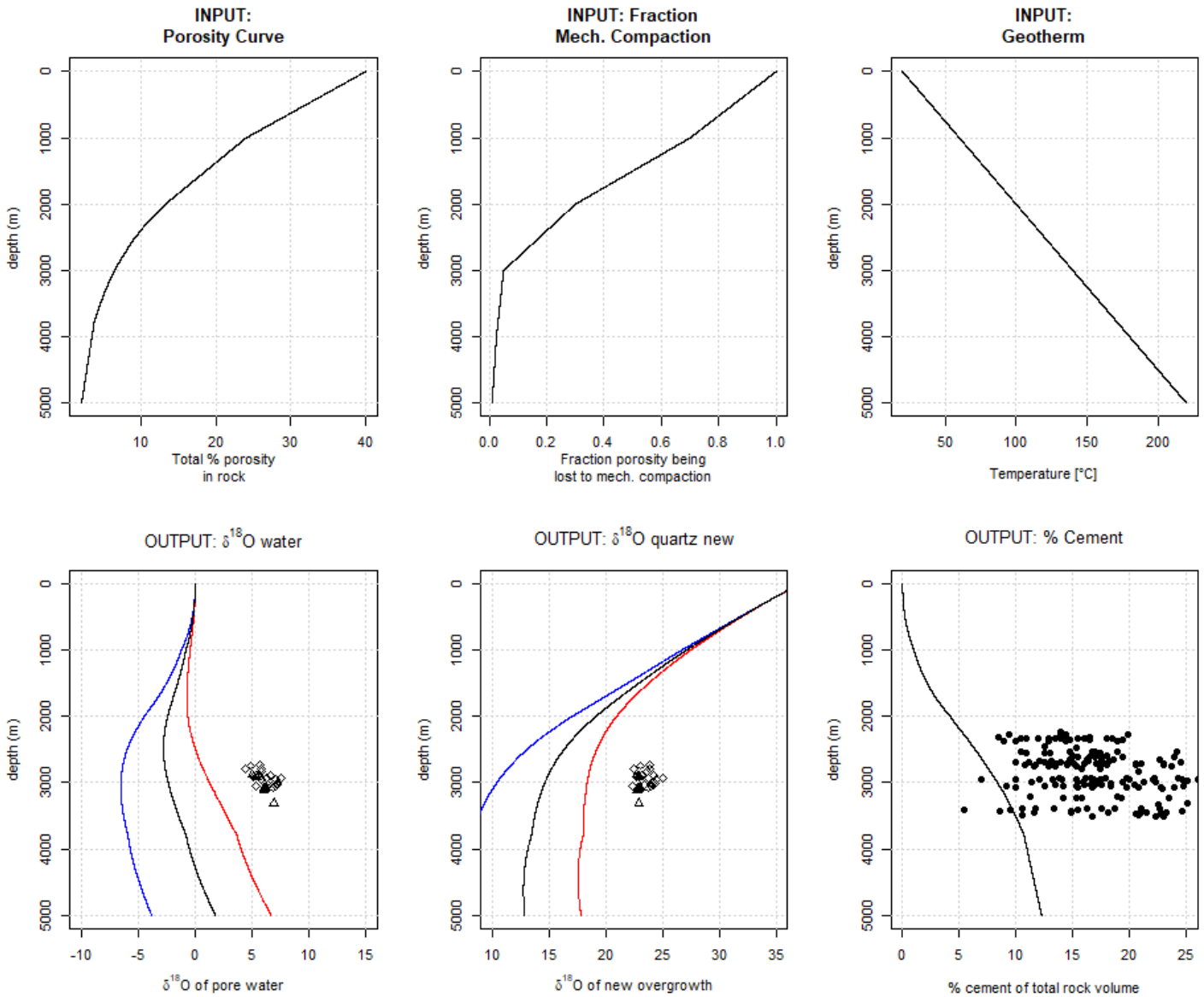
- **BLACK** => init_wat_d18o = 0‰
- **BLUE** => init_wat_d18o = 10‰ (evaporative brines)
- **RED** => init_wat_d18o = -10‰ (meteoric water)



Initial Quartz $\delta^{18}\text{O}$ Value ('init_detmin_d18o' parameter)

The $\delta^{18}\text{O}$ value of the detrital quartz grains can be set for a model run, and below is shown how changing this value to higher or lower initial $\delta^{18}\text{O}_{\text{qtz}}$ might affect the trajectory of porewater.

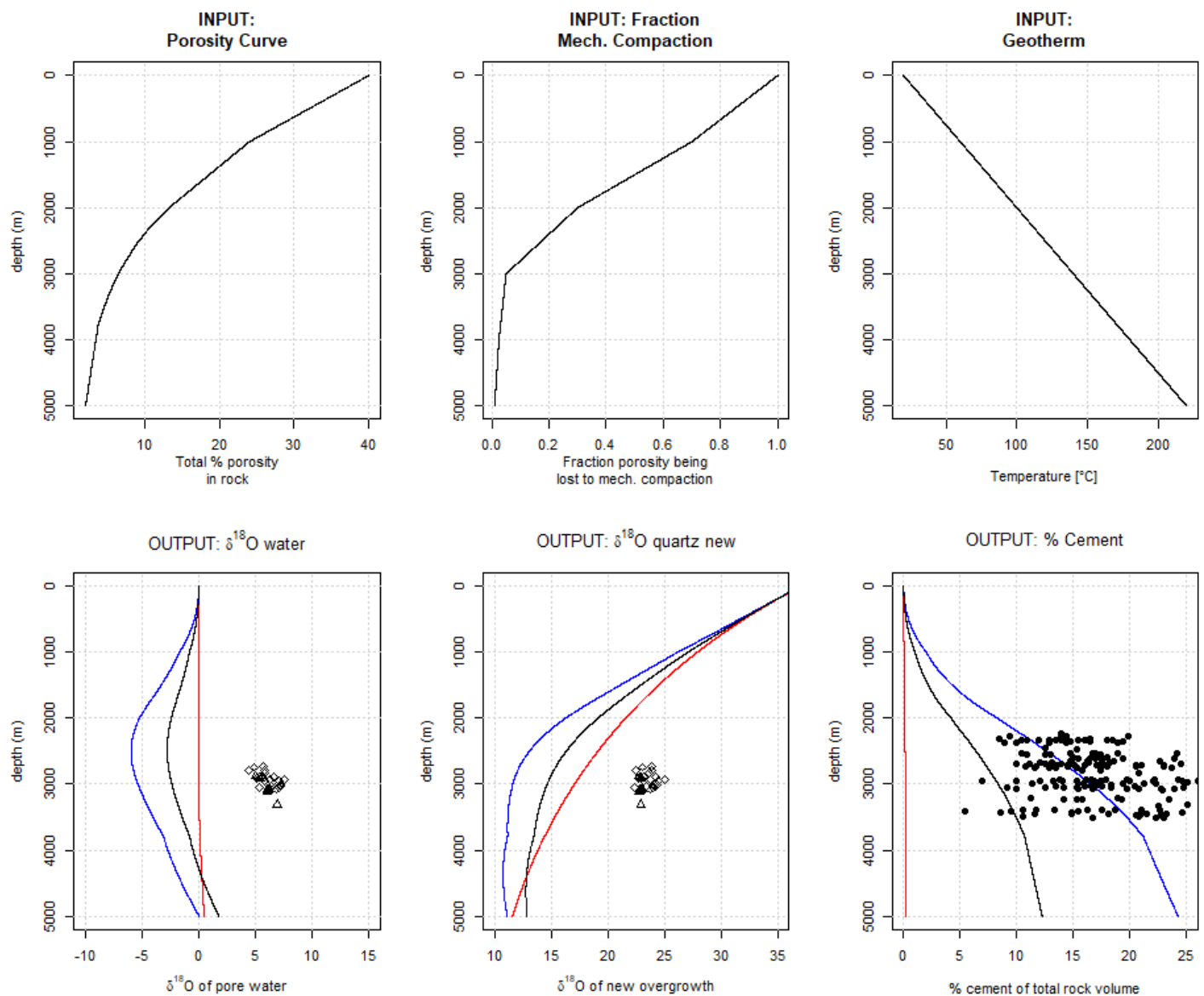
- **BLACK** => init_detmin_d18o = 13‰
- **BLUE** => init_detmin_d18o = 5‰ (anomalously low)
- **RED** => init_detmin_d18o = 20‰ (anomalously high)



Portion of Dissolving Cement vs. Dissolving Detrital Quartz ('cem_diss_prop' parameter)

In the model, a simplifying assumption needs to be made about the portion of overgrowth quartz that gets redissolved during pressure solution, relative to detrital quartz. In the spatial context of a sandstone, it might be argued that pressure solution silica sources are biased towards overgrowth cement, as this coats detrital grains and is therefore likely to be the first quartz phase to make grain-grain contact; however, determining this ratio geometrically throughout burial is challenging. In order to test the sensitivity of porewater to this unknown, a factor was introduced to represent the portion of dissolved quartz that is contributed from overgrowth sources. This factor is held constant throughout burial; the default value for this parameter is 0.5 (detrital and overgrowth quartz make equal contributions dissolved silica), but may take on a value between 0 and 1. Below are two examples of how this parameter changes the shape of the curve.

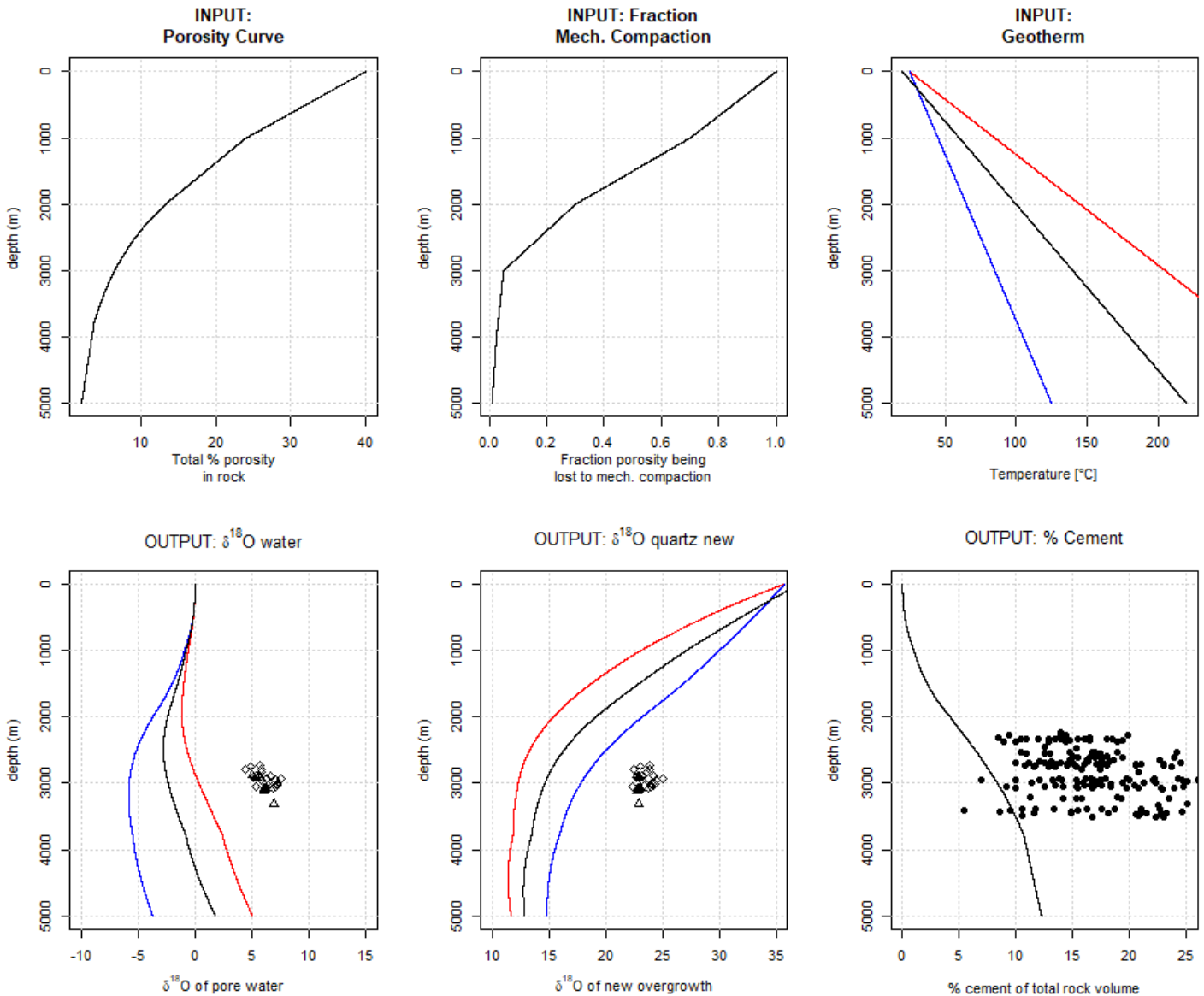
- **BLACK** => cem_diss_prop = 0.5 (default, pressure solution silica derived equally from detrital and overgrowth quartz)
- **BLUE** => cem_diss_prop = 0.01 (nearly all pressure solution silica derived from detrital quartz)
- **RED** => cem_diss_prop = 0.99 (nearly all pressure solution silica derived from overgrowth quartz)



Geothermal Gradient ('INPUT_geotherm' parameter)

The greatest effect that geothermal gradient has on model outputs is in determining the value of $\delta^{18}\text{O}_{\text{quartz}}$, due to the sensitivity of the quartz-water fractionation to temperature. Because of how the model is constructed (with no assumptions made about quartz precipitation kinetics), the geothermal gradient has no effect on % cement volume.

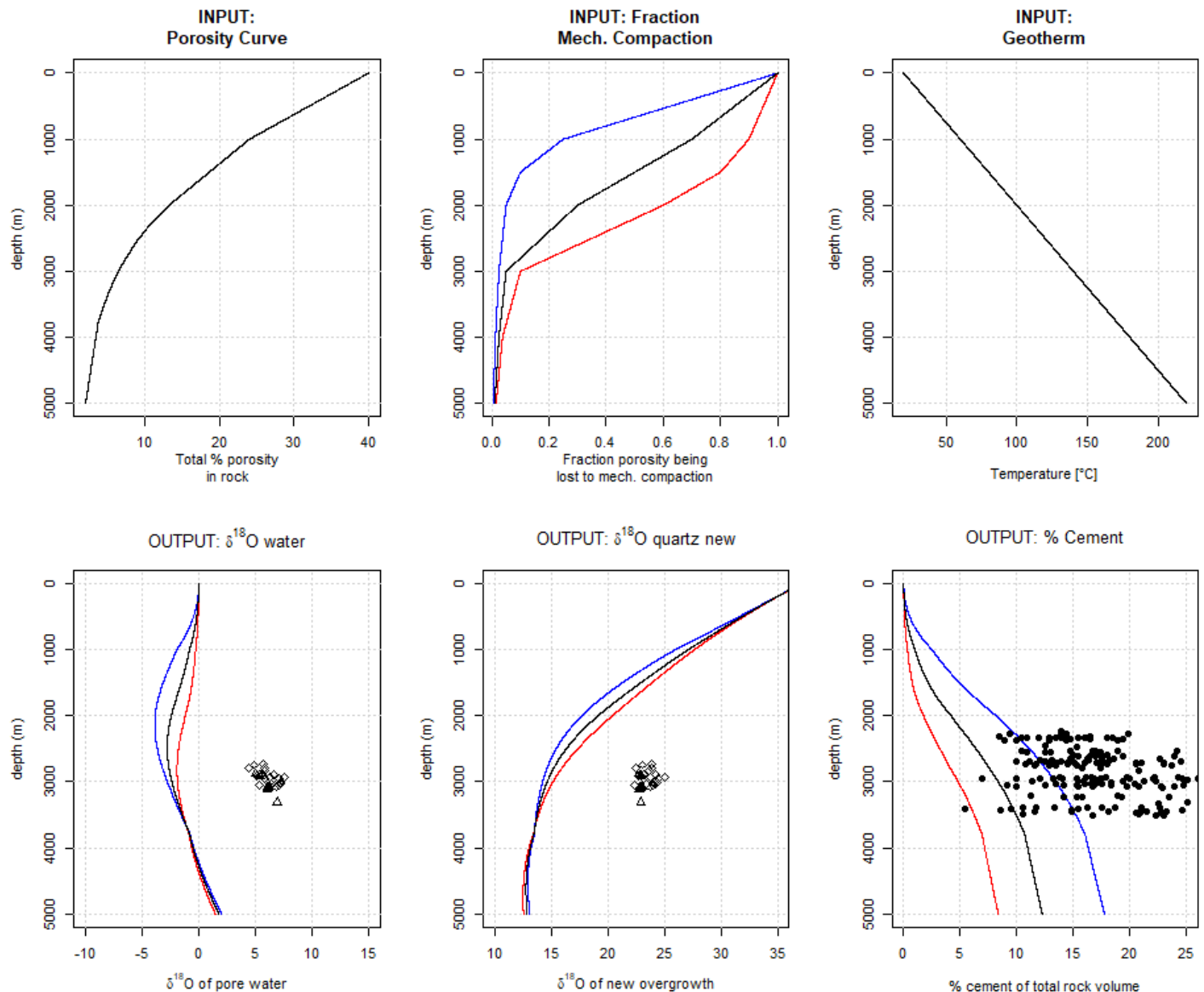
- **BLACK** => INPUT_geotherm = 40°C/km (default)
- **BLUE** => INPUT_geotherm = 20°C/km (cool geotherm)
- **RED** => INPUT_geotherm = 60°C/km (very hot geotherm)



Mechanical Compaction and Pressure Solution of Quartz ('INPUT_mech' parameter)

Of the three burial curve inputs (porosity, contribution of mechanical compaction to porosity change, and the geotherm), the greatest amount of model uncertainty probably arises from the mechanical compaction term. The reason for this is twofold. First, it is difficult to define the proportion of mechanical compaction that occurred in a rock with high precision at most depths. Second, the zone in which mechanical compaction is replaced by the processes of pressure solution and cementation falls in most sandstones in the 0.5 to 2 km range, where large changes in porosity are still underway, magnifying potential errors in the initial assumptions regarding rates of mechanical compaction.

To illustrate this sensitivity, the model has been run with two additional potential burial curves: one in which subsurface mechanical compaction contributes less to porosity loss (early initiation of cementation, **blue line**), and one in which subsurface mechanical compaction contributes more (late initiation of cementation, **red line**).

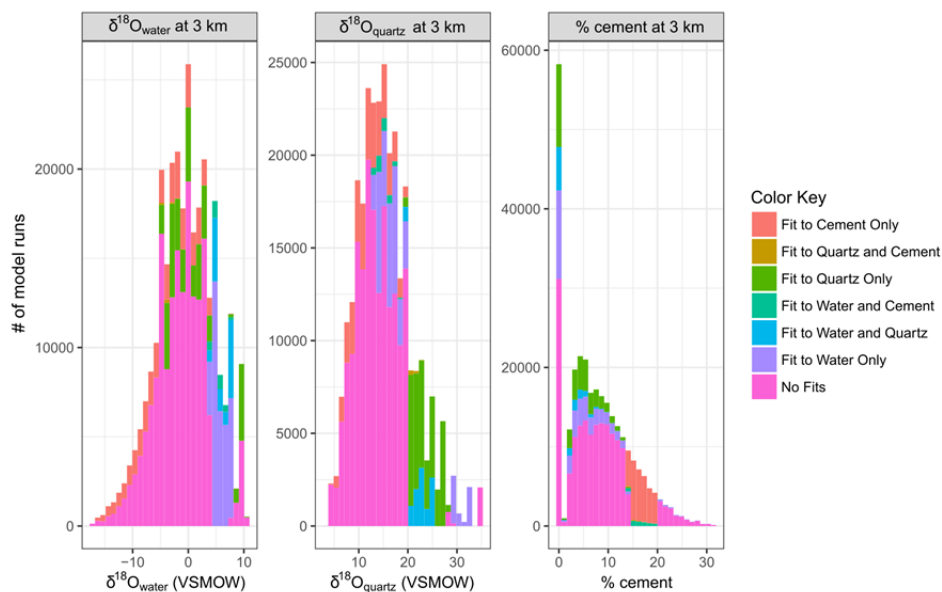


No Matches Found for All Possible Closed-System Conditions

For the depth range 0-3km, the model was tested iteratively through all reasonable sets of inputs to see if any could produce a match. These inputs were as follows:

- 1 constant porosity loss curve, described previously and derived from data by Dutton and Diggs (1992)
- 416 possible mechanical contribution curves, generated with the following limitations:
 - Mechanical contribution is changed in 0.1 increments
 - 2 possible mechanical contribution values at 0 km depth, ranging from 0.9 to 1
 - 10 possible mechanical contribution values at 1 km depth, ranging from 0 to 0.9
 - 9 possible mechanical contribution values at 2 km depth, ranging from 0 to 0.8
 - 8 possible mechanical contribution values at 3 km depth, ranging from 0 to 0.7
 - Mechanical contribution values at any depth cannot be greater than more shallow values (mechanical contribution cannot increase with depth)
- 4 geotherms of 20, 40, 60, and 80°C/km
- 1 initial surface temperature of 20°C
- 7 values for initial $\delta^{18}\text{O}_{\text{porewater}}$, at -5, -2.5, 0, 2.5, 5, 7.5, and 10‰
- 5 values for detrital grain $\delta^{18}\text{O}$, at 8, 10.5, 13, 15.5, and 18‰
- 5 values for the cement dissolution parameter, at 0.01, 0.25, 0.5, 0.75, and 0.99

This resulted in a total of 291,200 permutations of the model inputs, of which varied mechanical contribution curves were the greatest contributor. To speed computation, these models were all run with a 10 m burial increment, which shows minimal deviation in results from smaller depth increments (see the “Depth Increment” section above). The resulting curves output by the model were then classified as “Fit” to a given dataset if, at a depth of 3000 m, the output for $\delta^{18}\text{O}_{\text{porewater}}$ (by SIMS and FIA analysis) was between 4 and 8‰, the output for $\delta^{18}\text{O}_{\text{quartz}}$ (as compared to SIMS) was between 20 and 28‰, and if the output for % cement was between 14 and 20%. Of the 291,200 model runs, no simultaneous matches to all three datasets were registered (see histograms below).



Matches to all three datasets can be achieved if pressure solution begins unreasonably early (mechanical contribution < 0.5 at 0 km), detrital grains are unreasonably heavy (>18‰), and porewater is also initially unreasonably heavy (>5‰). As each of these inputs is considered to be highly unlikely given our current understanding of quartz cement precipitation and data from the Travis Peak Formation, this combination of input conditions is considered untenable by the authors.